JOURNAL OF MECHANICAL ENGINEERING AND SCIENCES (JMES)
ISSN: 2289-4659 e-ISSN: 2231-8380
VOL. 16, ISSUE 4, 2022, 9187 – 9196
DOI: https://doi.org/10.15282/jmes.16.4.2022.04.0728

ORIGINAL ARTICLE

The study on the influences of residual stresses on fatigue crack propagation in titanium alloy specimens

A. Zangeneh[1], I. Sattarifar[1,*], M. Noghabi[2]

[1] Department of Mechanical Engineering, Amirkabir University of Technology, No. 350, Hafez Ave, Valiasr Square, 1591634311, Tehran, Iran
Phone: +9866405844; Fax: +9866419736
[2] Iran Space Institute, No. 182, Shahid Teymuri Blvd., Tarasht, 1459777511,Tehran, Iran

ABSTRACT – Fatigue crack growth is a harmful physical phenomenon in engineering materials that can be intensified by the presence of tensile residual stresses. In the present study, the effect of tensile residual stresses on the fatigue crack growth in single-edge notched bending specimens of Ti- 6Al-4V is studied. Mechanical residual stresses were created by applying a 4-point bending process. The residual stresses were evaluated utilizing the hole drilling approach under the ASTM E-837 standard. Fatigue crack propagation was measured by experimental test in specimens with and without initial residual stresses. A finite element analysis was conducted using commercial finite element software to study the plastic zone at the crack tip and fracture mechanic parameters. It was observed that the residual stress field is redistributed after each step of crack propagation. The tensile residual stress in front of the crack tip decreased from near yield strength to approximately 30% of yield strength. The tensile residual stresses near the yield strength in Ti-6Al-4V increased the fatigue crack propagation rate by approximately 50%.

ARTICLE HISTORY
Received: 17th June 2022
Revised: 04th Nov. 2022
Accepted: 29th Oct. 2022
Published: 27th Dec. 2022

KEYWORDS
Fatigue crack growth
Residual stress
Titanium alloy
J-Integral

INTRODUCTION

Fatigue life is an essential dynamic feature of structures. Residual stresses in the crack front have a considerable effect on this feature. Fatigue life assessment with the presence of residual stresses remains a challenge for design engineers in different materials. Residual stresses can be obtained through manufacturing processes such as forming and welding, which, if they were not considered in the design of a structure, may result in failure while working. Compressive residual stress normal to crack face can delay crack propagation in both static and fatigue loading, while tensile residual stress will accelerate the fatigue crack propagation rate [1]. In this respect, many efforts have been put to measure residual stress magnitude and distribution in a structure to be considered in the fatigue design of a structure. Owunna et al. [2]evaluated welding residual stresses in TIG welding process from experimental and FEM approach. Metal forming can be defined as manufacturing metal parts and objects through solely mechanical deformation [3]. During reshaping the metal, mass is unchanged, and any material is not removed nor added to the base metal. Metal forming will result in residual stress distribution in the material, whose magnitude and distribution depend on the procedure. Four-point bending is a simple and common forming method that will induce both tensile and compressive residual stresses in a specimen.

For propagation of the crack, sufficient localized shear stress is needed which can be obtained by sufficient crack front opening displacement [4]. The presence of residual stresses will affect this procedure by accelerating or delaying the crack growth rate. In recent decades, numerous studies investigate the effect of residual stresses on fatigue crack growth rate. Farrahi et al. [4] have studied the influence of residual stresses induced by shot pinning and indentation method on crack tip closure and propagation behavior. They showed that delaying crack propagation and crack tip closure depend on the residual stress field, and compressive residual stresses will decrease the fatigue crack propagation rate. The compressive residual stresses can also be induced through cold expansion which has been used by Semari et al. on aluminum alloys [5]. They observed that having a higher value in compressive residual stresses, which can be achieved by different rates of cold expansion, will result in lower fatigue crack growth rates. Wahab et al. conducted a study on the effect of compressive residual stresses induced by an overload on the fatigue crack growth rate of aluminum specimens [6]. Their results indicated that overload will lead to a delay in the crack propagation rate. A study on the capability of linear-elastic fracture mechanics and superposition principle to determine fatigue crack growth rate was conducted by Stuart et al. [7]. They conducted their experimental tests on specimens with residual stresses, which were induced by cold expansion. Vempati et al. [8] studied the fatigue life of Ti-6Al-4V cruciform welded joints using XFEM. They investigated welded joints with various weld shapes and sizes to estimate the fatigue life of joints.

In most studies, the plastic zone formation in the crack front zone and also redistribution of residual stresses after fatigue cyclic loading and their effect on fatigue crack growth were not appropriately investigated. Considering the point that residual stresses are one of the secondary stresses and differ from primary stresses, which are results of external loading [9], the effects of each stress were considered in the calculation separately. Noghabi et al. [10] investigated the redistribution of residual stresses during fatigue crack growth in aluminum alloy CT specimens. They found that the residual stresses are mainly released during the first steps of fatigue loading. The authors also showed that Considering

*CORRESPONDING AUTHOR | I. Sattarifar | ✉ sattari@aut.ac.ir

the relaxation of initial residual stresses leads to conservative estimation of the fatigue life in engineering components [11]. Neto et al. numerically studied CT specimens submitted to single overloads and a high-strength material showed relatively small overload-affected zones. In this study, the comparison of numerical results with and without contact of crack flanks showed that crack closure is responsible for the effect of overloads on FCG rate behaviour [12].

A lot of industries are interested in methods, which increase the strength of specimens and slow down the fatigue crack propagation rate. Many efforts have been put to increase the strength of specimens. Nagaraja et al. [13] studied the effect of heat treatment and reinforcements on the tensile characteristics of an aluminium composite. Sharath et al. [14] investigated the improvement of wear characterization of an aluminium composite. There are several methods such as applying overload (OL) [15], indentation techniques [16], cold expansion process [17], laser shock peening [18], shot peening [19], water and oil jet peening [20], spot heating [21], and stop drilling holes [22] to arrest fatigue propagation and increase fatigue life of structures. Although many studies have been conducted to analyze the fatigue crack growth behaviour in the presence of residual stresses but, redistribution of residual stresses during fatigue crack propagation is still not clearly shown for most materials especially titanium alloys which the usage in the industry is rapidly increasing. The present research studies the influences of residual stresses field resulting from a 4-point bending method on fatigue crack growth behavior. Single Edge Notched bending (SENB) specimens of Ti-6Al-4V were used. The tensile residual stress field was located in front of the fatigue crack tip. The incremental hole-drilling approach was utilized to measure the residual stresses in accordance with ASTM E837 [23]. Employing the correlation displacement method and calculation of J-integral in the front of the crack tip, the values of the crack tip intensity factor were measured separately in each step of fatigue crack growth. Finally, the value of crack growth rate (da/dN) was measured by experimental tests, which will result in the fatigue crack growth parameter of Ti-6Al-4V.

Estimation of stress intensity factors using displacement-based approaches needs quarter-point finite elements in the first layer of mesh around the fractured head and substantial near-tip mesh enhancement. The displacement-based approaches are often less accurate than the J-integral or the stiffness derivative approach, but the accuracy level is enough for most applications [24]. The displacement-based approaches were mostly developed in the 1970s and 1980s by proposing a variety of special ‘‘quarter-point’’ finite elements [25]. Few new approaches were developed on the displacement-based approaches in the intervening years [26]. The displacement correlation method uses the finite element results of displacement from the nodes behind the crack tip to compute the stress intensity factor K. The effective K can be computed for each fatigue crack length at the corresponding applied loads Pmax and Pmin. The nodes normal to the crack face and behind the crack tip should be selected for the calculation of the effective K as a function of the distance to the crack tip. The effective stress intensity factor was calculated from the nodal displacements, according to [27]:

$$K = \frac{E\,u}{4(1-\nu^2)}\sqrt{\frac{2\Pi}{r}} \tag{1}$$

where, E is the Young modulus, ν is the Poisson’s ratio, r is the distance between the crack head to the node, and u is the displacement at the node position along with the crack head growth direction.

Mostly, the effective K for the nodes close to the crack tip shows an unstable behavior due to the pre-existing residual plastic strains. Disregarding the results for the first nodes close to the crack tip [27], the effective stress intensity factors can be found by extrapolation back to the crack head with a linear fit of the nodes at a higher r/a ratio.

THE MODIFIED J-INTEGRAL

The J contour integral is a successful method for characterizing the parameter of the fracture for nonlinear materials. By equivalenting elastic-plastic deformations as nonlinear elastic, Rice [28] developed fracture mechanics for nonlinear applications. Rice developed a path-independent contour integral for crack analysis. the value of this integral, as the J-integral, is equal to the energy release rate in a nonlinear cracked elastic body. of course, J is a more general form of the energy release rate. In the case of a linear elastic material [29],

$$J = \frac{K_I^2}{E'} \tag{2}$$

In order to estimate the quantity of J, assume a random clockwise path (Γ) around the head of a crack, as shown in Figure 1. The J-integral can be achieved by

$$J = \int_{\Gamma} (W\delta_{1i} - \sigma_{ij}\frac{\partial u_i}{\partial x_1})n_i ds \tag{3}$$

In which W is the density of strain energy, Ti is the traction vector component, ui is the displacement vector component, and ds is the incremental length along the contour Γ.

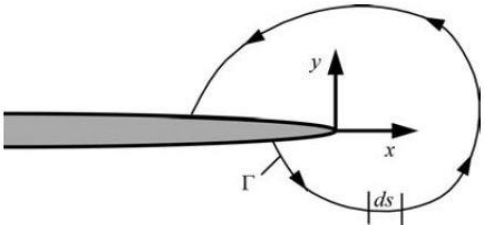

Figure 1. Arbitrary contour around the tip of a crack [16]

To estimate J-integral with finite element, it needs to be converted to a numerical integral. A common method for the mentioned conversion is Gauss Quadrature. By applying this method to Eq. (3) [30], the following equations are obtained.

$$J = \sum_{p=1}^{n_{total}} \sum^{n_g} \left\{ \left[\left(\sigma_{ij} \frac{\partial u_i}{\partial x_i} - W^m \delta_{ij} \right) \frac{\partial q_1}{\partial x_i} \right] det \left(\frac{\partial x_k}{\partial \eta_k} \right) \right\} w_p \tag{4}$$

$$J = \sum_{p=1}^{n_{total}} \sum^{n_g} \left\{ \left[\left(\sigma_{ij} \frac{\partial u_i}{\partial x_i} - W^m \delta_{ij} \right) \frac{\partial q_1}{\partial x_i} + \sigma_{ij} \frac{\partial \varepsilon_{ij}^0}{\partial x_1} \right] det \left(\frac{\partial x_k}{\partial \eta_k} \right) \right\} w_p \tag{5}$$

where, n_{total} is the number of total elements, n_g is the number of Gaussian integral nodes in each element, and w_p is weight functions.

SPECIMEN PREPARATION AND FATIGUE TESTS

To measure da/dN, Fatigue crack growth tests with constant amplitude were conducted on SENB specimens, according to ASTM E647 [31]. Specimens dimensions and boundary conditions are specified in Figure 2. All tests were conducted with a hydraulic fatigue testbed with a frequency of 10 Hz in ambient temperature. Specimens with and without mechanical residual stresses were tested. Under ASTM E647, to assure that the notch is sharp enough, a pre-crack was created with fatigue cyclic loading. 1 mm pre-crack creation required 12000 cycles with R = 0.1.

After pre-crack formation, a 3-point bending procedure was used until the failure of the sample to determine the critical load. The critical load can also be calculated with Eqs. (6) and (7).

$$P_{cr} = 1.072\, \eta\, B\, b\, \sigma_y \qquad (\text{Plain stress}) \tag{6}$$

$$P_{cr} = 1.455\, \eta\, B\, b\, \sigma_y \qquad (\text{Plain strain}) \tag{7}$$

In Eqs. (6) and (7), B is the sample thickness, b is the specimen width, and η is a geometrical constant as follows,

$$\eta = \sqrt{\left(\frac{2a}{b}\right)^2 + \frac{4a}{b} + 2} - \left(\frac{2a}{b} + 1\right) \tag{8}$$

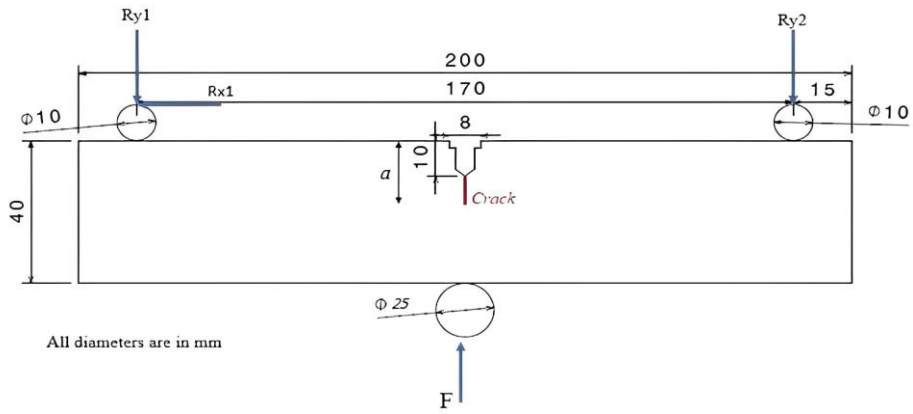

Figure 2. Dimensions and boundary conditions of SENB specimen

FINITE ELEMENT ANALYSIS

SENB specimen was simulated in a finite element commercial software based on Figure 2. Material properties were defined as elastic-plastic isotropic hardening behavior based on Ti-6Al-4V mechanical properties, which were measured by tensile strength test (Table 1). Due to the symmetrical simulation, only one-quarter of the sample was simulated in finite element analysis.

Table 1. Mechanical properties of Ti-6Al-4V

Property	Yield strength (MPa)	Ultimate strength (MPa)	Young's module (GPa)	Poisson's ratio
Value	950	1030	113.8	0.3

In Figure 3, the meshing process is demonstrated. 4-node elements with reduced integral nodes CPE4R were used for meshing. As is shown in Figure 3, the elements closer to the crack face are smaller (50 μm) than in other zones. To create singularity ability for the elements in the crack front, elements in the mentioned zone were converted to a singular quarter-point element which is proposed by Abdelaziz et al [32].

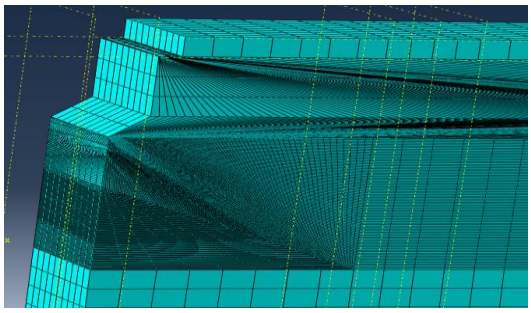

Figure 3. Meshing procedure with smaller mesh size near the crack front

Mechanical Residual Stresses Induction

A 4-point bending simulation was designed to induce tensile residual stresses in front of the crack front. The boundary conditions that were used for SENB specimen were according to Figure 4. To induce residual stresses, a compressive 6 KN load (F) was applied to the pins. By applying the load, the zones near the crack front will experience plastic deformation. Consequently, after unloading, there will be a plastic residual strain, which will result in residual stresses. The residual stress contour is demonstrated in Figure 5 after unloading.

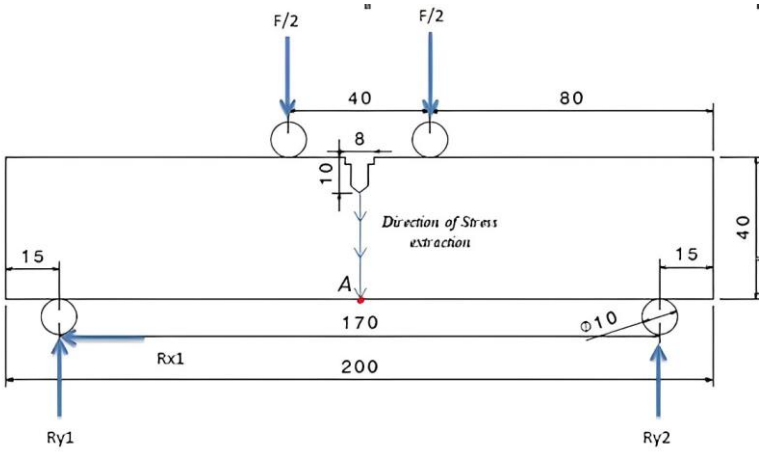

Figure 4. Dimensions and boundary conditions of 4-point bending

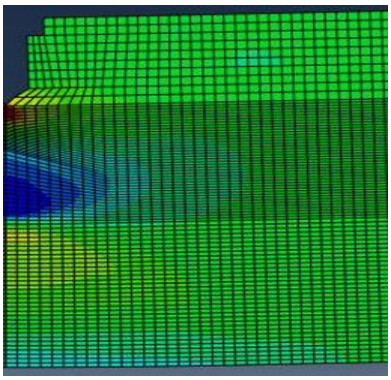

Figure 5. Residual stress field after unloading

In Figure10, the magnitude of induced residual stresses versus distance from the crack front is indicated. The horizontal axis indicates the distance along the crack growth direction. As is shown, the residual stress field is tensile near the crack front zone and turns compressive by moving along the crack growth direction. Crack growth was simulated in each step by releasing the crack tip node. One of the most crucial points in node release is time. The time of node release can be at minimum load, maximum load, or a little after maximum load [33]. In the case of small enough elements near the crack tip, releasing time of nodes will not affect the results [34]. In this study, node release happened at minimum load after two cycles of fatigue loading.

J-Integral Calculations

Concerning relatively large areas of plastic deformation created near the crack tip, elastoplastic fracture mechanics can present a better understanding of crack growth behavior, which is illustrated by Eq. (9) [35],

$$\Delta J = \Delta J_{el} + \Delta J_{pl} = \frac{\Delta K^2}{E'} + \frac{\eta A_{pl}}{B b_0} \tag{9}$$

where, b_0 is the primary specimen ligament, B is the specimen width, W is the effective specimen width, A_{pl} is the area under load-displacement plot, and η is a dimensionless coefficient.

In the current simulation, the crack front consisted of 10 nodes (normal to the crack face along with the thickness of the specimen). The value of *J*-integral is calculated for each node separately. This simulation is carried out for the different lengths of crack from 1.5 mm to 9 mm with 0.5 mm crack growth in each step. The value of *J*-integral is demonstrated in Figure 6 for 3 mm crack with and without residual stresses.

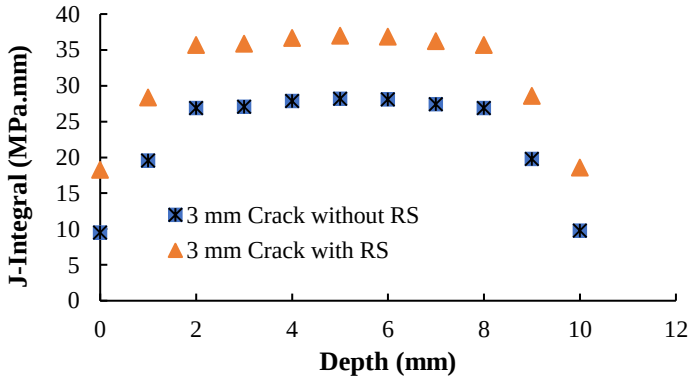

Figure 6. Value of J-integral

Stress Intensity Factor Calculations

Irwin suggested Eq. (10) to estimate the plastic zone radius around the crack tip. If the plastic zone radius around the crack tip is smaller than r_y, then the value of the stress intensity factor can be estimated from *J*-integral [29].

$$r_y = \frac{1}{2\Pi}\left(\frac{K_I}{\sigma_y}\right) \tag{10}$$

The radius of the plastic zone determined for the longest crack (9 mm) is 1.51 mm, which is 20% lower than r_y. Consequently, SIFs can be calculated from Eq. (11) [16].

$$J = \frac{K^2}{E'} \quad where \;\; E' = \frac{E}{1-\nu} \;\; for\ plane\ stress \tag{11}$$

The values of SIFs calculated from *J*-integral are shown in Figure 8 for the 3 mm crack with and without residual stresses. SIFs can also be calculated directly by the displacement correlation method, which is demonstrated for the 3 mm crack in Figure 7. By using Eq. (1) for each node, the value of SIFs can be calculated. As is shown in Figure 9, SIFs were converged into a constant value which is SIF for 3 mm crack.

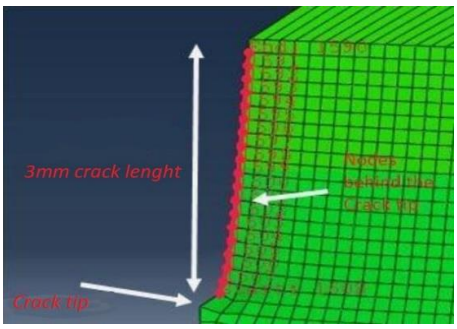

Figure 7. Displacement correlation method for SIFs calculation

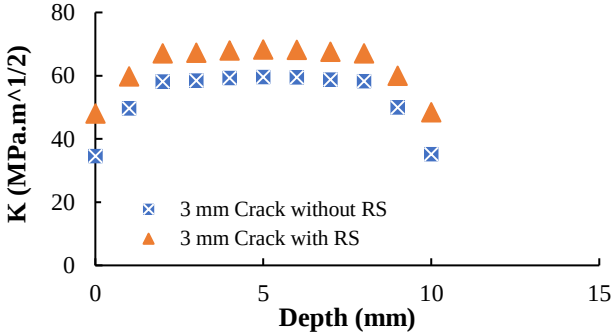

Figure 8. Values of SIFs calculated from J-integral

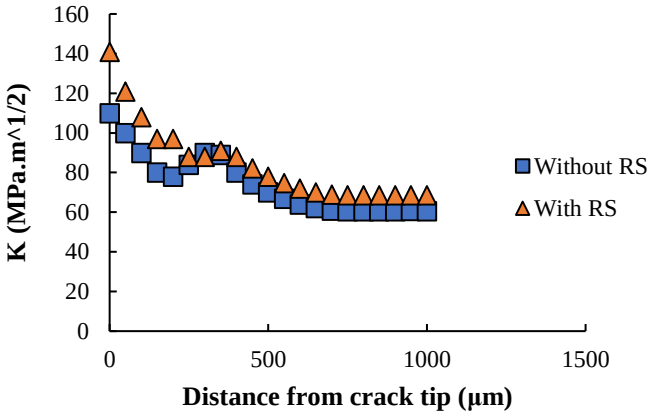

Figure 9. Values of SIFs calculated from displacement correlation method

EXPERIMENTAL STUDY

Material and Specimens

Ti-6Al-4V titanium alloy was used in the experiment. The study was conducted on SENB samples with a thickness of 10 mm and 40 mm in width. The mechanical properties of the specimens are presented in Table 1. There were two groups of specimens: those with mechanical residual stresses and those without residual stresses.

Residual Stress Measurement

Measurement of residual stresses was carried out by the incremental hole-drilling approach. Strain gauge rosettes manufactured by Tokyo Measuring Instruments Laboratory Co., Ltd., QFRA-1-11 with a rosette diameter of 5.13 mm were used. A high-speed air turbine was employed to drill the hole with a diameter of 2 mm. The incremental depth of incremental drilling was 0.1 mm. According to ASTM E-837, the measured strains can be converted to residual stresses. In this procedure, it is assumed that the magnitude of residual stress is not dependent on the thickness of specimens, which will result in only near-surface measurement. The measurement was carried out after the creation of a 1mm fatigue pre-crack. Based on the results of FEM analysis of the residual stress field, three points with the distance of 9 mm,19 mm, and 26 mm from the pre-crack tip were chosen to validate the FEM analysis which is demonstrated in Figure 10.

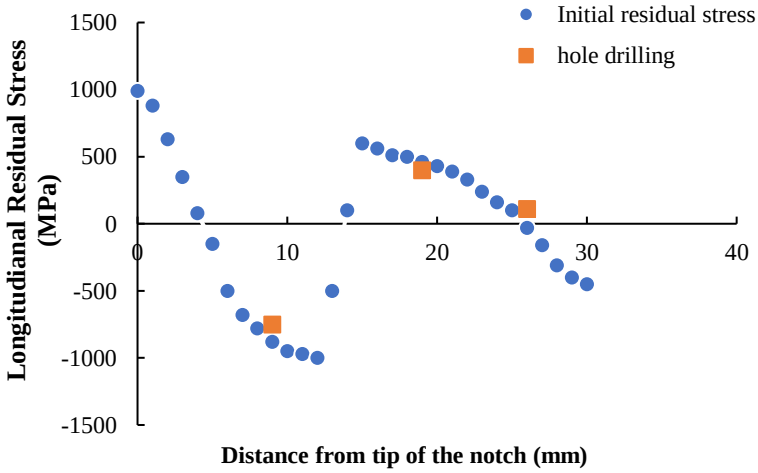

Figure 10. Residual stress measurement

Fatigue Tests

Measurement of fatigue crack growth was conducted according to ASTM E-647, which included cyclic loading on notched specimens, which are already pre-cracked. The number of cycles was measured in each 0.5 mm increment of crack growth. The final growth of the crack was 9 mm. Sinusoidal cyclic loading was applied in the form of 3-point bending on SENB specimen with a frequency of 10 Hz. This test was carried out on four specimens, two of them with mechanical residual stresses and the other two without residual stresses. The average result of the two specimens' crack length versus the number of cycles is plotted in Figure 11. The results presented in Figure 11 are in agreement with Lee et al. [36], which observed similar results (Figure 12).

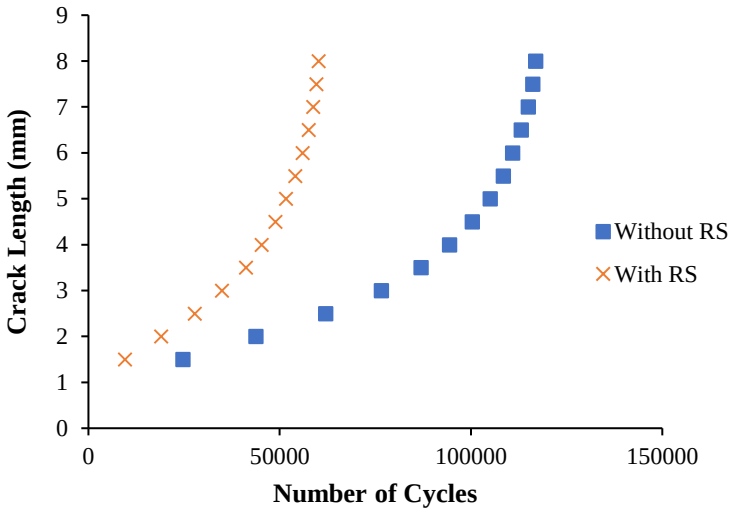

Figure 11. Comparison of crack growth length

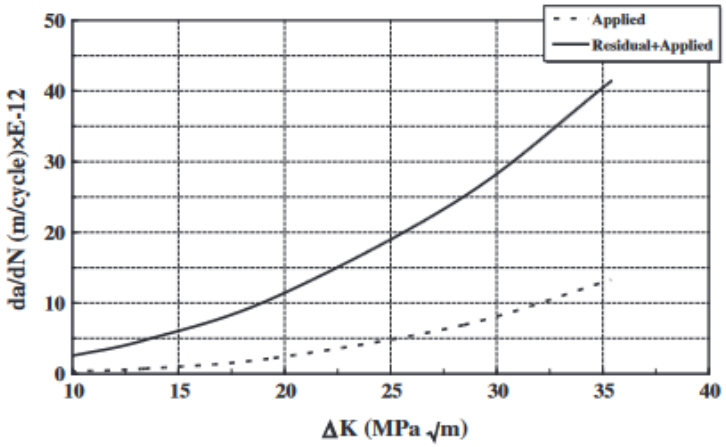

Figure 12. Comparison of fatigue crack growth rate in specimens wirh and without residual stress [36]

DISCUSSIONS

The magnitude of tensile residual stresses was measured in front of 1 mm pre-crack tip which is close to Ti-6Al-4V yield strength. By applying cyclic fatigue loading, the results portend that the residual stresses were released as they decreased to 30% of the yield strength after 4 mm crack growth. The residual stress magnitude in the distance of 1 mm in front of the crack head for each 0.5 mm crack growth is demonstrated in Figure 13. This result is in good agreement with the study conducted by Larue et al. [37] on 2024-T351 aluminum alloy specimens, who concluded that residual stresses would have a diminished impact when they are reduced to 25% of the yield strength of the material. Their results are shown in Figure 14.

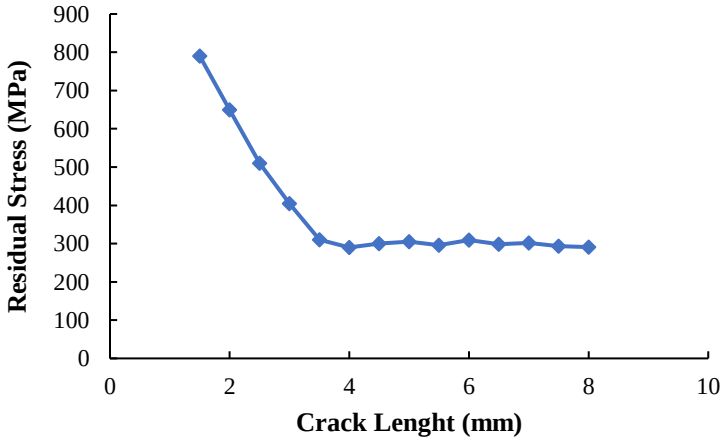

Figure 13. Values of residual stresses in the distance of 1 mm from the crack tip

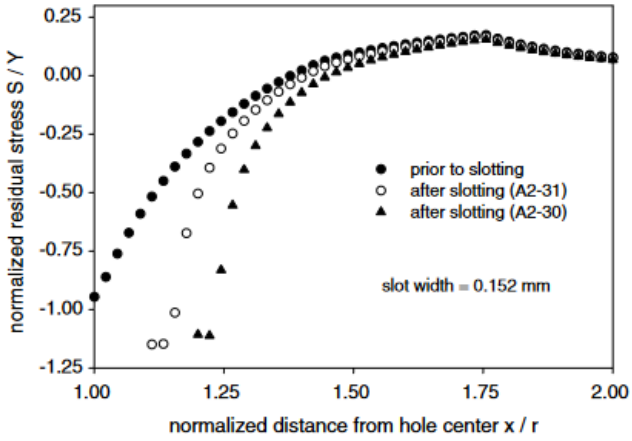

Figure 14. Residual stress results from finite element simulation [37]

Fatigue Crack Growth Rate Measurement

By using the data in Figure 11, the fatigue crack growth is characterized using ΔK which is shown in Figure 15. The results showed that above ΔK = 70 MPa.m^1/2, the fatigue crack propagation rate for the specimen without residual stresses and the specimen with tensile residual stresses would be converged. fatigue crack growth rate increase due to the existence of tensile residual stresses in front of the crack tip is clearly shown in Figure 15. The results also indicated that after 3.5 mm crack growth, the residual stresses are no longer effective in the value of fatigue crack growth rate. The value of crack growth rate for a constant ΔK was determined in Table 2. As it is calculated, the difference between crack growth rate for samples with and without residual stresses was decreased from 48% to 4.5% which is proof of residual stress relaxation after applying cyclic loading. These results are in good agreement with the results obtained in [10]. The results obtained from the literature [10] are shown in Figure 16.

Table 2. Fatigue crack growth rate

*ΔK (*MPa.m^1/2)	Crack growth rate da/dN (mm/cycle)		Difference (%)
	Without residual stresses	With residual stresses	
51	2.74003E-05	5.27825E-05	48
71	8.51999E-05	9.579818E-05	11
99	2.68091E-04	2.56051E-04	4.5

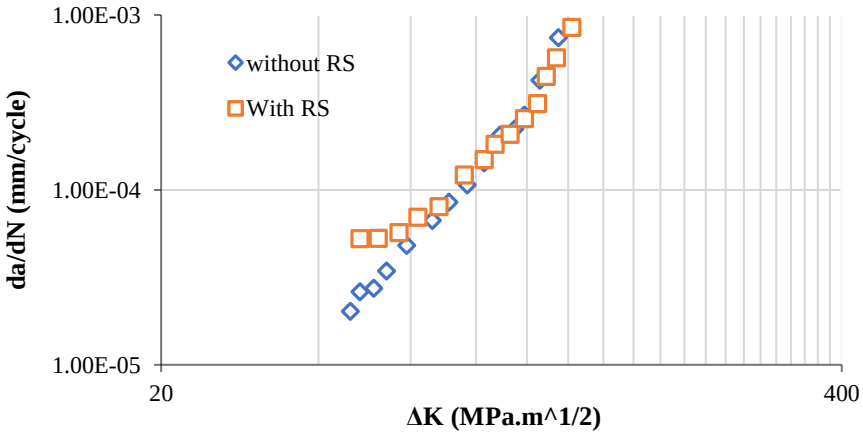

Figure 15. Crack growth rate versus ΔK

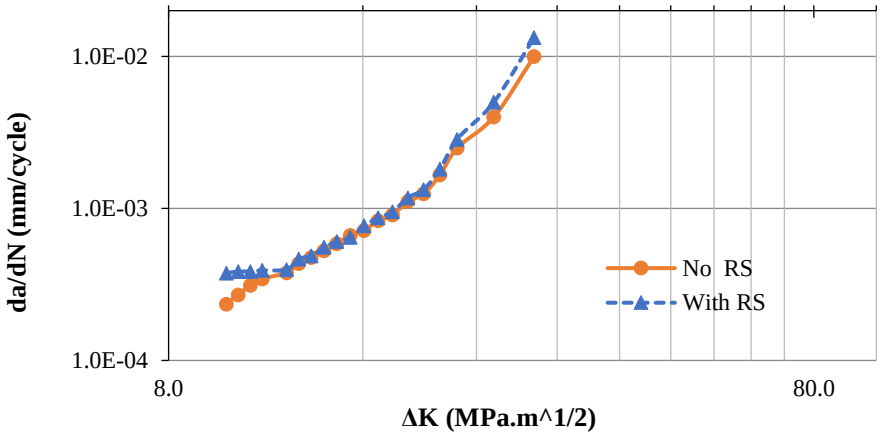

Figure 16. Fatigue crack growth rate versus ΔK [10]

CONCLUSIONS

In the present study, the effect of tensile residual stresses on fatigue crack growth in single-edge notched bending specimens of Ti-6Al-4V was studied. Mechanical residual stresses were created by applying a 4-point bending process. The values of SIFs were calculated using the modified J-integral method both with and without residual stresses, and the following conclusions were achieved.

1. The stress intensity factor calculated using the J-integral and displacement correlation method showed relatively good agreement. Hence, due to a more straightforward calculation, the displacement correlation method can be used instead of the calculation based on the J-integral.
2. The radius of the plastic zone increased with each step of fatigue crack growth. Although, it always remained lower than r_y (1.5 mm).
3. The residual stress field is redistributed after each step of crack propagation. The tensile residual stress in front of the crack tip decreased from near yield strength to approximately 30% of yield strength.
4. The tensile residual stresses near the yield strength in Ti-6Al-4V increased the fatigue crack propagation rate by approximately 50%.
5. The fatigue crack propagation rate was found to be converged with the rate of the specimen without residual stresses after the relaxation of residual stresses.
6. If the Paris law is used to predict the crack growth rate for a specimen with residual stresses, a conservative design will be achieved.

REFERENCES

[1] G. H. Farrahi, J. L. Lebrijn, and D. Couratin, "Effect of shot peening on residual stress and fatigue life of a spring steel," *Fatigue & Fracture of Engineering Materials & Structures*, vol. 18, no. 2, pp. 211–220, 1995.

[2] I. B. Owunna and A. E. Ikpe, "Evaluation of induced residual stresses on AISI 1020 low carbon steel plate from experimental and FEM approach during TIG welding process," *Journal of Mechanical Engineering and Sciences*, vol. 13, no. 1, pp. 4415–4433, 2019.

[3] R. H. Wagoner and J.-L. Chenot, *Fundamentals of Metal Forming*. Wiley, 1996.

[4] G. H. Farrahi, G. H. Majzoobi, F. Hosseinzadeh, and S. M. Harati, "Experimental evaluation of the effect of residual stress field on crack growth behaviour in C(T) specimen," *Engineering Fracture Mechanics*, vol. 73, no. 13, pp. 1772–1782, 2006.

[5] Z. Semari, A. Aid, A. Benhamena, A. Amrouche, M. Benguediab, A. Sadok and N. Benseddiq, "Effect of residual stresses induced by cold expansion on the crack growth in 6082 aluminum alloy," *Engineering Fracture Mechanics*, vol. 99, pp. 159–168, 2013.

[6] M. A. A. Wahab, G. R. R. Rohrsheim, and J. H. H. Park, "Experimental study on the influence of overload induced residual stress field on fatigue crack growth in aluminium alloy," *Journal of Materials Processing Technology*, vol. 153–154, pp. 945–951, 2004.

[7] D. H. Stuart, M. R. Hill, and J. C. Newman, "Correlation of one-dimensional fatigue crack growth at cold-expanded holes using linear fracture mechanics and superposition," *Engineering Fracture Mechanics*, vol. 78, no. 7, pp. 1389–1406, 2011.

[8] S. R. Vempati, K. B. Raju, and K. V. Subbaiah, "Simulation of Ti-6Al-4V cruciform welded joints subjected to fatigue load using XFEM," *Journal of Mechanical Engineering and Sciences*, vol. 13, no. 3, pp. 5371–5389, 2019.

[9] EN 13445-3, Unfired Pressure Vessels—Part 3: Design, *European Committee for Standardization Brussels*, Belgium, 2002.

[10] M. Noghabi, I. Sattari-far, and H. H. Toudeshky, "The study of redistribution in residual stresses during fatigue crack growth," *Journal of Mechanical Engineering and Sciences*, vol. 15, no. 4, pp. 8565–8579, 2021.

[11] M. Noghabi, I. Sattarifar, and H. Hosseini-Toudeshky, "The study on the overloading effect on fatigue crack growth considering residual stress relaxation in Al 5456-H38," *Mechanics Based Design of Structures and Machines*, pp. 1–20, 2022.

[12] D. M. Neto, M. F. Borges, F. V. Antunes, and J. Jesus, "Mechanisms of fatigue crack growth in Ti-6Al-4V alloy subjected to single overloads," *Theoretical and Applied Fracture Mechanics*, vol. 114, p. 103024, 2021.

[13] S. Nagaraja, R. Kodandappa, K. Ansari, M. S. Kuruniyan, A. Afzal, A. R. Kaladgi *et al.*, "Influence of heat treatment and reinforcements on tensile characteristics of aluminium AA 5083/silicon carbide/fly ash composites," *Materials*, vol. 14, no. 18, p. 5261, 2021.

[14] B. N. Sharath, C. V. Venkatesh, A. Afzal, N. Aslfattahi, A. Aabid, M. Baig and B. Saleh, "Multi ceramic particles inclusion in the aluminium matrix and wear characterization through experimental and response surface-artificial neural networks.," *Materials (Basel)*, vol. 14, no. 11, 2021.

[15] H. Wang, J. Zhang, Y. Li, Z. Wang, and J. Wu, "Experimental investigation of overload effects on fatigue crack growth behaviour of 7050-T7451 aluminium alloy," *Fatigue and Fracture of Engineering Materials and Structures*, vol. 43, pp. 1–15, 2020.

[16] P. S. Song and G. L. Sheu, "Retardation of fatigue crack propagation by indentation technique," *International Journal of Pressure Vessels and Piping*, vol. 79, no. 11, pp. 725–733, 2002.

[17] R. Ghfiri, A. Amrouche, I. Abdellatif, and G. Mesmacque, "Fatigue life estimation after crack repair in 6005 A-T6 aluminum alloy using the cold expansion hole technique," *Fatigue and Fracture of Engineering Materials and Structures*, vol. 23, no. 11, pp. 911–916, 2000.

[18] E. Hombergsmeier, V. Holzinger, and U. C. Heckenberger, "Fatigue crack retardation in LSP and SP treated aluminium specimens," *Advanced Materials Research*, vol. 891–892, pp. 986–991, 2014.

[19] Y. Mutoh, G. H. Fair, B. Noble, and R. B. Waterhouse, "The effect of residual stresses induced by shot-peening on fatigue crack propagation in two high strength aluminium alloys," *Fatigue and Fracture of Engineering Materials and Structures*, vol. 10, no. 4, pp. 261–272, 1987.

[20] D. Odhiambo and H. Soyama, "Cavitation shotless peening for improvement of fatigue strength of carbonized steel," *International Journal of Fatigue*, vol. 25, no. 9–11, pp. 1217–1222, 2003.

[21] B. B. Verma and P. K. Ray, "Fatigue crack growth retardation in spot heated mild steel sheet," *Bulletin of Materials Science*, vol. 25, no. 4, pp. 301–307, 2002.

[22] H. Wu, A. Imad, N. Benseddiq, J. Tupiassu Pinho de Castro, and M. Antonio Meggiolaro, "On the prediction of the residual fatigue life of cracked structures repaired by the stop-hole method," *International Journal of Fatigue*, vol. 32, no. 4, pp. 670–677, 2010.

[23] ASTM E837, Standard Test Method for Determining Residual Stresses by the Hole-drilling Strain-gage Method, ASTM International, 2020.

[24] P. Fu, S. M. Johnson, R. R. Settgast, and C. R. Carrigan, "Generalized displacement correlation method for estimating stress intensity factors," *Engineering Fracture Mechanics*, vol. 88, pp. 90–107, 2012.

[25] P. P. Lynn and A. R. Ingraffea, "Transition elements to be used with quarter-point crack-tip elements," *International Journal for Numerical Methods in Engineering*, vol. 12, no. 6, pp. 1031–1036, 1978.

[26] L. Banks-Sills, "Application of the finite element method to linear elastic fracture mechanics," *Applied Mechanics Reviews*, vol. 44. no. 10. pp. 447-461, 1991.

[27] C. Garcia, T. Lotz, M. Martinez, A. Artemev, R. Alderliesten, and R. Benedictus, "Fatigue crack growth in residual stress fields," *International Journal of Fatigue*, vol. 87, pp. 326–338, 2016.

[28] J. R. Rice, "A path independent integral and the approximate analysis of strain concentration by notches and cracks," *Journal of Applied Mechanics*, vol. 35, no. 2, pp. 379–386, 1968.

[29] T. L. Anderson, *Fracture Mechanics: Fundamentals and Applications*, Third Edition, CRC Press, 2005.

[30] E. F. Rybicki and M. F. Kanninen, "A finite element calculation of stress intensity factors by a modified crack closure integral," *Engineering fracture mechanics*, vol. 9, no. 4, pp. 931–938, 1977.

[31] ASTM Standard E647 − 13a, "Standard Test Method for Measurement of Fatigue Crack Growth Rates," *American Society for Testing and Materials*, pp. 1–50, 2014.

[32] Y. Abdelaziz, S. Benkheira, T. Rikioui, and A. Mekkaoui, "A double degenerated finite element for modeling the crack tip singularity," *Applied Mathematical Modelling*, vol. 34, no. 12, pp. 4031–4039, 2010.

[33] K. Solanki and S. R. Daniewicz, "Finite element analysis of plasticity-induced fatigue crack closure : An overview," *Engineering Fracture Mechanics*, vol. 71, no. 2, pp. 149–171, 2004.

[34] K. Solanki, S. R. Daniewicz, and J. C. Newman, "Finite element modeling of plasticity-induced crack closure with emphasis on geometry and mesh refinement effects," *Engineering Fracture Mechanics*, vol. 70, no. 12, pp. 1475–1489, 2003.

[35] ASTM E1820, "Standard Test Method for Measurement of Fracture Toughness," *ASTM Book of Standards*, 2013.

[36] C. Lee and K. Chang, "Finite element computation of fatigue growth rates for mode I cracks subjected to welding residual stresses," *Engineering Fracture Mechanics*, vol. 78, no. 13, pp. 2505–2520, 2011.

[37] J. E. Larue and S. R. Daniewicz, "Predicting the effect of residual stress on fatigue crack growth," *International Journal of Fatigue*, vol. 29, no. 3, pp. 508–515, 2007.